Journal of Computational Physics 229 (2010) 8552–8563

Contents lists available at ScienceDirect

Journal of Computational Physics

journal homepage: www.elsevier.com/locate/jcp

Error analysis of a discontinuous Galerkin method for Maxwell equations in dispersive media ☆

Bo Wang [a], Ziqing Xie [a,*], Zhimin Zhang [b,c,1]

[a] College of Mathematics and Computer Science, Key Laboratory of High Performance Computing and Stochastic Information Processing, Ministry of Education of China, Hunan Normal University, Changsha, Hunan 410081, China
[b] College of Mathematics and Computational Science, Sun-Yat-sen University, Guangzhou, Guangdong 510275, China
[c] Department of Mathematics, Wayne State University, Detroit, MI 48202, USA

ARTICLE INFO

Article history:
Received 8 February 2010
Received in revised form 2 July 2010
Accepted 27 July 2010
Available online 5 August 2010

Keywords:
Discontinuous Galerkin method
Maxwell equations
Dispersive media
Plasma
Debye medium
Lorentz medium

ABSTRACT

A discontinuous Galerkin method for the numerical approximation of time-dependent Maxwell equations in three different dispersive media is introduced. Both the L^2-stability and error estimate of the DG method are discussed in detail. We show that the proposed method has an accuracy of $O(h^{k+\frac{1}{2}})$ under the L^2-norm when polynomials of degree k in space are used. Furthermore, numerical experiments are provided to justify our theoretical analysis.

1. Introduction

In recent years, growing attention has been paid to finite element methods in solving Maxwell equations [2,3,20,4,10,21,9,11,22,18]. Actually, finite element methods have been used for both time-harmonic and time-dependent Maxwell equations. However, majority works are restricted to simple media such as air in free space. Nevertheless, dispersive media are ubiquitous. Consequently, the study of how electromagnetic wave propagates in dispersive media becomes very important. More physical background about this area can be found in [14].

The discontinuous Galerkin methods (DG) are a class of finite element methods using discontinuous piecewise polynomials as trial and test functions. Although more degrees of freedom are needed in the implementation of DG methods to achieve the same order of accuracy, compared with the continuous finite element methods, the discontinuities at the element interfaces allow the design of suitable inter-element boundary treatments to obtain highly accurate and stable methods in many difficult situations. Actually they have several distinctive advantages, e.g., applicability for non-conforming mesh, high-order accuracy, flexibility in handling material interface and high parallelizability. We refer to the survey paper [1] and the review paper [7] and their references therein.

☆ Supported by the National Natural Science Foundation of China (10871066, 10571053), Programme for New Century Excellent Talents in University (NCET-06-0712).

* Corresponding author. Tel.: +86 13786146580; fax: +86 73188872867.
E-mail address: ziqingxie@yahoo.com.cn (Z. Xie).

1 This author is supported in part by the US National Science Foundation. under Grant DMS-0612908.

0021-9991/$ - see front matter © 2010 Elsevier Inc. All rights reserved.
doi:10.1016/j.jcp.2010.07.038

In [13], the first attempt was made to implement the finite element method for Maxwell equations in dispersive media. In the subsequent years, Li [14–17] did a series of works on this topic. Especially in [14], he proposed a fully discrete mixed finite element scheme for 3D Maxwell equations in three different dispersive media. In fact an edge element method was used to approximate the magnetic field **H**, and a DG method for the electric field **E**.

In 2000's, DG methods are among the most popular numerical approaches for Maxwell equations [4,10,21]. It is worthwhile to mention Cockburn, Li and Shu's work [6], which introduced a locally divergence-free DG method in solving Maxwell equations. The locally divergence-free restriction reduces the dimension of the finite element space and leads to a cheaper computational cost. In [18], Lu, Zhang, and Cai implemented a DG method for Maxwell equations in linear dispersive and lossy materials of Debye type with perfectly matched layer (PML) boundary conditions. However the L^2-stability and error analysis were missing. In [12], an IPDG method was used for the time-dependent Maxwell equations in cold plasma. The optimal error estimates in the energy norm were proved.

In this paper, we follow the approach in [6] by using the locally divergence-free DG method in space to solve Maxwell equations in dispersive media. The resulting integro–differential equations from the space discretization are solved by the continuous finite element method of degree k. Three important and useful dispersive media are considered. Both the L^2-stability and error estimate with order $k+\frac{1}{2}$ for the semi-discretization scheme are established when piecewise polynomials of degree k in space are used. Nevertheless, our numerical results show a $k+1$ – order accuracy, which are better than the theoretical result.

The outline of this paper is as follows. In Section 2, we introduce the model problem and its corresponding DG formulation. In Section 3, we discuss the L^2-stability and error estimate. How our approach works for three specific dispersive media is shown in Section 4. Numerical results are given in Section 5 to demonstrate the effectiveness of the proposed method. Possible future work and concluding remarks are presented in Section 6.

2. Model problem and DG formulation

In this section, we consider an unified model problem which is used to describe the electromagnetic wave propagation in three dispersive media by introducing a so-called polarization current J. Details about how to link three specific dispersive media to the unified form will be shown in Section 4. The unified model problem is

$$\mu\frac{\partial \mathbf{H}}{\partial t}+\nabla\times\mathbf{E}=0 \quad \text{in } \Omega\times(0,T_0], \tag{2.1}$$

$$\epsilon\frac{\partial \mathbf{E}}{\partial t}-\nabla\times\mathbf{H}+\mathbf{J}(\mathbf{E},t)=0 \quad \text{in} \quad \Omega\times(0,T_0], \tag{2.2}$$

where μ and ϵ are positive constants,

$$\mathbf{J}(\mathbf{E},t)=c\mathbf{E}+\int_0^t f(t-\tau)\mathbf{E}(\mathbf{x},\tau)d\tau, \tag{2.3}$$

is the polarization current, with c a nonnegative constant, and f a given function. It is worthwhile to point out that μ, ϵ, c and f are dependent on the media. Further, a perfect conduction boundary condition

$$\mathbf{n}\times\mathbf{E}=0 \quad \text{on } \partial\Omega\times(0,T_0] \tag{2.4}$$

and a simple initial condition

$$\mathbf{E}(\mathbf{x},0)=\mathbf{E}_0(\mathbf{x}),\quad \mathbf{H}(\mathbf{x},0)=\mathbf{H}_0(\mathbf{x}) \quad \text{in } \Omega, \tag{2.5}$$

are imposed, where $\mathbf{n}$ is the outward unit normal of $\partial\Omega$, $\mathbf{E}_0$ and $\mathbf{H}_0$ are given functions with $\mathbf{H}_0$ satisfying

$$\nabla\cdot(\mu\mathbf{H}_0)=0 \quad \text{in } \Omega,\quad \mathbf{H}_0\cdot\mathbf{n}=0 \quad \text{on } \partial\Omega. \tag{2.6}$$

We can easily obtain, from (2.1) and (2.6), that

$$\nabla\cdot(\mu\mathbf{H})=0,$$

which is the solenoidal condition of magnetic flux density. Furthermore, the second condition of (2.6), together with (2.1) and (2.2), leads to [20]

$$\mathbf{H}\cdot\mathbf{n}=0 \quad \text{on } \partial\Omega\times(0,T_0], \tag{2.7}$$

which is also a perfect conduct boundary condition.

Before defining the DG method, we introduce some notations and the locally divergence-free finite element space. We assume that Ω is decomposed by a regular tetrahedra mesh $\mathcal{T}_h$ with maximum diameter h. An element is denoted by K, a face by e, and the outward unit normal by $\mathbf{n}_K$. We also denote by $\mathcal{E}_\mathcal{I}$ the union of all interior faces of $\mathcal{T}_h$, by $\mathcal{E}_\mathcal{D}$ the union of all boundary faces of $\mathcal{T}_h$, and by $\mathcal{E}=\mathcal{E}_\mathcal{I}\bigcup\mathcal{E}_\mathcal{D}$ the union of all faces of $\mathcal{T}_h$. Let $P^k(K)$ denote the space of polynomials in K of degree at most k. The finite element space is given by

$$\mathbf{V}_h^k=\overline{\mathbf{V}}_{h,0}^k\bigoplus\overline{\mathbf{V}}_h^k,$$

where

$$\overline{\mathbf{V}}_h^k = \left\{ \mathbf{v} : \mathbf{v}|_K \in (P^k(K))^3, \quad K \in \mathcal{T}_h \right\},$$
$$\overline{\mathbf{V}}_{h,0}^k = \left\{ \mathbf{v} : \mathbf{v}|_K \in (P^k(K))^3 \quad \text{and} \quad \nabla \cdot \mathbf{v} = 0 \quad \text{in } K, \ K \in \mathcal{T}_h \right\},$$

are approximation spaces for the electric field $\mathbf{E}$ and the magnetic field $\mathbf{H}$, respectively. Note that vectors in $\overline{\mathbf{V}}_{h,0}^k$ are locally divergence-free.

Next, we introduce some trace operators on the interior faces. Let e be an interior face which belongs to element K. We define

$$\mathbf{v}^{int(K)}(\mathbf{x}) = \lim_{t \to 0-} \mathbf{v}(\mathbf{x} + t\mathbf{n}_K), \quad \mathbf{v}^{ext(K)}(\mathbf{x}) = \lim_{t \to 0+} \mathbf{v}(\mathbf{x} + t\mathbf{n}_K) \quad \forall \mathbf{x} \in e.$$

Then we define the average and tangential jump of $\mathbf{v}$ on any interior face e as follows:

$$\bar{\mathbf{v}} = \frac{\mathbf{v}^{int(K)} + \mathbf{v}^{ext(K)}}{2}, \quad [\mathbf{v}]_T = \mathbf{n}_K \times \mathbf{v}^{int(K)} - \mathbf{n}_K \times \mathbf{v}^{ext(K)}.$$

For a boundary face $e \subset \mathcal{E}_\mathcal{D}$ which belongs to element K, we define

$$\mathbf{v}^{int}(\mathbf{x}) = \mathbf{v}^{int(K)}(\mathbf{x}), \quad \forall \mathbf{x} \in e.$$

To define the DG formulation, we rewrite (2.1), (2.2) and (2.5) in the form

$$\mathbf{QU}_t + \nabla \cdot \mathbf{f}(\mathbf{U}) + \widehat{\mathbf{J}}(\mathbf{U}) = 0 \quad \text{in } \Omega \times (0, T_0], \tag{2.8}$$
$$\mathbf{U}(\mathbf{x}, 0) = \mathbf{U}_0(\mathbf{x}) \quad \text{in } \Omega, \tag{2.9}$$

where

$$\mathbf{U} = \begin{pmatrix} \mathbf{H} \\ \mathbf{E} \end{pmatrix}, \mathbf{U}_0 = \begin{pmatrix} \mathbf{H}_0 \\ \mathbf{E}_0 \end{pmatrix}, \quad \mathbf{Q} = \begin{pmatrix} \mu I_{3\times3} & 0_{3\times3} \\ 0_{3\times3} & \epsilon I_{3\times3} \end{pmatrix},$$
$$\mathbf{f}(\mathbf{U}) = [\mathbf{f}_1(\mathbf{U}), \mathbf{f}_2(\mathbf{U}), \mathbf{f}_3(\mathbf{U})]^T, \quad \mathbf{f}_i(\mathbf{U}) = \begin{pmatrix} \mathbf{e}_i \times \mathbf{E} \\ -\mathbf{e}_i \times \mathbf{H} \end{pmatrix},$$
$$\widehat{\mathbf{J}}(\mathbf{U}) = \begin{pmatrix} 0_{3\times1} \\ \mathbf{J}(\mathbf{E}, t) \end{pmatrix}.$$

Multiplying (2.8), (2.9) by test function $\mathbf{v} = [v_H, v_E]^T$, integrating over K, and performing the integration by parts, we have

$$\mathbf{Q} \int_K \mathbf{U}_t \cdot \mathbf{v} d\mathbf{x} + \int_{\partial K} (\mathbf{f}(\mathbf{U}) \cdot \mathbf{n}_K) \cdot \mathbf{v} ds - \int_K \mathbf{f}(\mathbf{U}) \cdot \nabla \mathbf{v} d\mathbf{x} + \int_K \widehat{\mathbf{J}}(\mathbf{U}) \cdot \mathbf{v} d\mathbf{x} = 0, \tag{2.10}$$
$$\int_K \mathbf{U}(\mathbf{x}, 0) \cdot \mathbf{v}(\mathbf{x}) d\mathbf{x} = \int_K \mathbf{U}_0 \cdot \mathbf{v}(\mathbf{x}) d\mathbf{x}. \tag{2.11}$$

Motivated by the DG method for Maxwell equations in [6], the DG formulation based on (2.10), (2.11) is to find $\mathbf{U}_h \in \mathbf{V}_h^k$, such that

$$\mathbf{Q} \int_K \frac{\partial}{\partial t} \mathbf{U}_h \cdot \mathbf{v}_h d\mathbf{x} + \sum_{e \subset \partial K} \int_e \mathbf{h}(\mathbf{U}_h^{ext(K)}, \mathbf{U}_h^{int(K)}, \mathbf{n}_K) \cdot \mathbf{v}_h ds - \int_K \mathbf{f}(\mathbf{U}_h) \cdot \nabla \mathbf{v}_h d\mathbf{x} + \int_K \widehat{\mathbf{J}}(\mathbf{U}_h) \cdot \mathbf{v}_h d\mathbf{x} = 0, \tag{2.12}$$

$$\int_K \mathbf{U}_h(\mathbf{x}, 0) \cdot \mathbf{v}_h d\mathbf{x} = \int_K \mathbf{U}_0(\mathbf{x}) \cdot \mathbf{v}_h d\mathbf{x}. \tag{2.13}$$

Here we choose the numerical flux $\mathbf{h} = \mathbf{h}(\mathbf{U}_h^{ext(K)}, \mathbf{U}_h^{int(K)}, \mathbf{n}_K)$ as the up-winding one, i.e., on an interior face $e \subset \mathcal{E}_\mathcal{I}$,

$$\mathbf{h}(\mathbf{U}_h^{ext(K)}, \mathbf{U}_h^{int(K)}, \mathbf{n}_K) = \begin{pmatrix} \mathbf{n}_K \times \left(\overline{\mathbf{E}}_h - \frac{1}{2} [\mathbf{H}_h]_T\right) \\ -\mathbf{n}_K \times \left(\overline{\mathbf{H}}_h + \frac{1}{2} [\mathbf{E}_h]_T\right) \end{pmatrix} \tag{2.14}$$

and on a boundary face $e = \partial K \bigcap \mathcal{E}_\mathcal{D}$,

$$\mathbf{h}(\mathbf{U}_h^{ext(K)}, \mathbf{U}_h^{int(K)}, \mathbf{n}_K) = \begin{pmatrix} \mathbf{0}_{3\times1} \\ -\mathbf{n}_K \times \left(\mathbf{H}_h^{int(K)} + \mathbf{n}_K \times \mathbf{E}_h^{int(K)}\right) \end{pmatrix}, \tag{2.15}$$

which is consistent with $\mathbf{f}(U) \cdot n_K$.

After the space discretization, we obtain the following system of Volterra integro–differential equations

$$\mathbf{A} \frac{d\mathbf{U}_h(t)}{dt} + \mathbf{B}\mathbf{U}_h(t) + \mathbf{C} \int_0^t f(t - \tau) \mathbf{U}_h(\tau) d\tau = 0 \quad t \in (0, T_0], \tag{2.16}$$

with initial condition

$$\mathbf{U}_h(0) = \mathbf{P}_h(\mathbf{U}_0), \tag{2.17}$$

where **A**, **B** and **C** are coefficient matrices independent of t. In order to obtain a fully discrete formula, we have to discretize this system of integro–differential equations. In this paper, the continuous finite element method is used to discretize (2.16) and (2.17). Let $0 = t_0 < t_1 < \cdots < t_n = T_0$ be a triangulation of the interval $[0,T_0]$ with elements denoted by $I_j = [t_j,t_{j+1}]$, $j = 0,1,\ldots,n-1$. The time discretization scheme is to find

$$\mathbf{U}_{h,j}(t) = \sum_{i=0}^{k} \mathbf{U}_{h,j}^{i}\psi_j^i(t) \quad t \in I_j, \tag{2.18}$$

such that

$$\mathbf{A}\int_{I_j} \frac{d\mathbf{U}_{h,j}(t)}{dt} v(t)dt + \mathbf{B}\int_{I_j} \mathbf{U}_{h,j}(t)v(t)dt + \mathbf{C}\int_{I_j} \mathbf{M}_j(t)v(t)dt = 0 \quad v \in P^{k-1}(I_j), \tag{2.19}$$

$$\mathbf{U}_{h,0}^0 = \mathbf{P}_h(\mathbf{U}_0), \quad \mathbf{U}_{h,j}^0 = \mathbf{U}_{h,j-1}^k, \quad j = 1,2,\ldots,k, \tag{2.20}$$

where $\psi_j^i(t), i = 0,1,\ldots,k$ are the Lagrange interpolation basis functions of degree k on interval I_j and

$$\mathbf{M}_j(t) = \int_{t_j}^{t} f(t-\tau)\mathbf{U}_{h,j}(\tau)d\tau + \sum_{i=1}^{j-1}\int_{I_i} f(t-\tau)\mathbf{U}_{h,i}(\tau)d\tau,$$

where the integrals can be calculated by Gauss–Legendre quadrature formula.

3. L^2-stability and error estimates

In this section, we will investigate the L^2-stability and error estimate of the DG scheme described in Section 2. We start with defining a bilinear form based on the weak formulation (2.12). For this purpose, summing up (2.12) over K in $\mathcal{T}_h$, and integrating in t from 0 to T, we obtain

$$B_h(\mathbf{U}_h,\mathbf{v}_h;T) = 0 \quad \forall \mathbf{v}_h(.,t) \in \mathbf{V}_h^k, \quad \forall t \in (0,T), \quad \forall T \in (0,T_0], \tag{3.1}$$

where

$$\begin{aligned} B_h(\mathbf{U}_h,\mathbf{v}_h;T) = &\int_0^T\int_\Omega (\mu\partial_t\mathbf{H}_h(\mathbf{x},t)\cdot\mathbf{v}_{h,\mathbf{H}}(\mathbf{x},t) + \epsilon\partial_t\mathbf{E}_h(\mathbf{x},t)\cdot\mathbf{v}_{h,\mathbf{E}}(\mathbf{x},t))d\mathbf{x}dt + \int_0^T\sum_{K\in\mathcal{T}_h}\sum_{e\subset\partial K}\int_e \mathbf{h}(\mathbf{U}_h^{ext(K)},\mathbf{U}_h^{int(K)},\mathbf{n}_K) \\ &\cdot\mathbf{v}_h(\mathbf{x},t)dsdt - \int_0^T\int_\Omega \mathbf{f}(\mathbf{U}_h)\cdot\nabla\mathbf{v}_h(\mathbf{x},t)d\mathbf{x}dt + \int_0^T\int_\Omega \mathbf{J}(\mathbf{E_h},t)\cdot\mathbf{v}_{h,\mathbf{E}}(\mathbf{x},t)d\mathbf{x}dt. \end{aligned} \tag{3.2}$$

Next, we derive an expression for $B_h(\mathbf{U}_h,\mathbf{U}_h;T)$.

Lemma 3.1. *For any $\mathbf{U}_h(\cdot,t) \in \mathbf{V}_h^k$, $t \in (0,T)$, and $T \in (0,T_0]$, we have*

$$\begin{aligned} B_h(\mathbf{U}_h,\mathbf{U}_h;T) = &\frac{1}{2}(\mu\|\mathbf{H}_h(\mathbf{x},T)\|^2 + \epsilon\|\mathbf{E}_h(\mathbf{x},T)\|^2) + \frac{1}{2}\Theta_{T,T_h}(\mathbf{U}_h) + \int_0^T\int_\Omega \mathbf{J}(\mathbf{E_h},t)\cdot\mathbf{E}_h(\mathbf{x},t)d\mathbf{x}dt - \frac{1}{2}(\mu\|\mathbf{H}_h(\mathbf{x},0)\|^2 \\ &+ \epsilon\|\mathbf{E}_h(\mathbf{x},0)\|^2), \end{aligned} \tag{3.3}$$

where

$$\Theta_{T,T_h}(\mathbf{U}_h) = \int_0^T\sum_{e\subset\mathcal{E}_\mathcal{I}}\int_e |[\mathbf{H}_h(\mathbf{x},t)]_T|^2 + |[\mathbf{E}_h(\mathbf{x},t)]_T|^2 dsdt + 2\int_0^T\sum_{e\subset\mathcal{E}_\mathcal{D}}\int_e |\mathbf{n}\times\mathbf{E}_h^{int}|^2 dsdt.$$

Proof. Setting $\mathbf{v}_h = \mathbf{U}_h$ in (3.2), we get

$$\begin{aligned} B_h(\mathbf{U}_h,\mathbf{U}_h;T) = &\frac{1}{2}(\mu\|\mathbf{H}_h(\mathbf{x},T)\|^2 + \epsilon\|\mathbf{E}_h(\mathbf{x},T)\|^2) - \frac{1}{2}(\mu\|\mathbf{H}_h(\mathbf{x},0)\|^2 + \epsilon\|\mathbf{E}_h(\mathbf{x},0)\|^2) + \int_0^T\sum_{K\in\mathcal{T}_h}\sum_{e\subset\partial K}\int_e \mathbf{h}(\mathbf{U}_h^{ext(K)},\mathbf{U}_h^{int(K)},\mathbf{n}_K) \\ &\cdot\mathbf{U}_h(\mathbf{x},t)dsdt - \int_0^T\int_\Omega \mathbf{f}(\mathbf{U}_h)\cdot\nabla\mathbf{U}_h(\mathbf{x},t)d\mathbf{x}dt + \int_0^T\int_\Omega \mathbf{J}(\mathbf{E_h},t)\cdot\mathbf{E}_h(\mathbf{x},t)d\mathbf{x}dt. \end{aligned}$$

We only need to show

$$\frac{1}{2}\Theta_{T,T_h}(\mathbf{U}_h) = \int_0^T\sum_{K\in\mathcal{T}_h}\sum_{e\subset\partial K}\int_e \mathbf{h}(\mathbf{U}_h^{ext(K)},\mathbf{U}_h^{int(K)},\mathbf{n}_K)\cdot\mathbf{U}_h(x,t)dsdt - \int_0^T\int_\Omega \mathbf{f}(\mathbf{U}_h)\cdot\nabla\mathbf{U}_h(\mathbf{x},t)d\mathbf{x}dt. \tag{3.4}$$

Actually,

$$\begin{aligned}\int_0^T\int_\Omega \mathbf{f}(\mathbf{U}_h)\cdot\nabla\mathbf{U}_h(\mathbf{x},t)d\mathbf{x}dt &= \int_0^T\sum_{K\in\mathcal{T}_h}\int_K\left(\sum_{i=1}^3 e_i\times\mathbf{E}_h^{int(K)}\cdot\frac{\partial}{\partial x_i}\mathbf{H}_h^{int(K)}-\sum_{i=1}^3 e_i\times\mathbf{H}_h^{int(K)}\cdot\frac{\partial}{\partial x_i}\mathbf{E}_h^{int(K)}\right)d\mathbf{x}dt\\ &= \int_0^T\sum_{K\in\mathcal{T}_h}\int_K\sum_{i=1}^3\left(\frac{\partial}{\partial x_i}(e_i\times\mathbf{E}_h^{int(K)}\cdot\mathbf{H}_h^{int(K)})-e_i\times\frac{\partial}{\partial x_i}\mathbf{E}_h^{int(K)}\cdot\mathbf{H}_h^{int(K)}\right)d\mathbf{x}dt\\ &\quad-\int_0^T\sum_{K\in\mathcal{T}_h}\int_K\sum_{i=1}^3 e_i\times\mathbf{H}_h^{int(K)}\cdot\frac{\partial}{\partial x_i}\mathbf{E}_h^{int(K)}d\mathbf{x}dt\\ &= \int_0^T\sum_{K\in\mathcal{T}_h}\sum_{e\subset\partial K}\int_e \mathbf{n}_K\times\mathbf{E}_h^{int(K)}\cdot\mathbf{H}_h^{int(K)}dsdt.\end{aligned}$$

Then direct calculation leads to

$$\begin{aligned}&\int_0^T\sum_{K\in\mathcal{T}_h}\sum_{e\in\partial K}\int_e \mathbf{h}(\mathbf{U}_h^{ext(K)},\mathbf{U}_h^{int(K)},\mathbf{n}_K)\cdot\mathbf{U}_h(\mathbf{x},t)dsdt-\int_0^T\int_\Omega\mathbf{f}(\mathbf{U}_h)\cdot\nabla\mathbf{U}_h(\mathbf{x},t)d\mathbf{x}dt\\ &=\int_0^T\sum_{K\in\mathcal{T}_h}\sum_{e\subset\partial K\bigcap\mathcal{E}_\mathcal{I}}\int_e\left(\mathbf{n}_K\times\overline{\mathbf{E}}_h\cdot\mathbf{H}_h^{int(K)}-\frac{1}{2}\mathbf{n}_K\times[\mathbf{H}_h]_T\cdot\mathbf{H}_h^{int(K)}\right)dsdt\\ &\quad+\int_0^T\sum_{K\in\mathcal{T}_h}\sum_{e\subset\partial K\bigcap\mathcal{E}_\mathcal{I}}\int_e\left(-\mathbf{n}_K\times\overline{\mathbf{H}}_h\cdot\mathbf{E}_h^{int(K)}-\frac{1}{2}\mathbf{n}_K\times[\mathbf{E}_h]_T\cdot\mathbf{E}_h^{int(K)}\right)dsdt\\ &\quad-\int_0^T\sum_{K\in\mathcal{T}_h}\int_{\partial K\bigcap\mathcal{E}_\mathcal{D}}\left(\mathbf{n}\times\mathbf{H}_h^{int(K)}\cdot\mathbf{E}_h^{int(K)}-|\mathbf{n}\times\mathbf{E}_h^{int(K)}|^2\right)dsdt-\int_0^T\sum_{K\in\mathcal{T}_h}\int_{\partial K\bigcap\mathcal{E}_\mathcal{D}}\mathbf{n}\times\mathbf{E}_h^{int(K)}\cdot\mathbf{H}_h^{int(K)}dsdt\\ &\quad-\int_0^T\sum_{K\in\mathcal{T}_h}\sum_{e\in\partial K\bigcap\mathcal{E}_\mathcal{I}}\int_e\mathbf{n}\times\mathbf{E}_h^{int(K)}\cdot\mathbf{H}_h^{int(K)}dsdt=I_1+I_2+I_3+I_4+I_5.\end{aligned}\tag{3.5}$$

It is obvious that

$$I_3+I_4=\int_0^T\sum_{e\subset\mathcal{E}_\mathcal{D}}\int_e\left|\mathbf{n}\times\mathbf{E}_h^{int}\right|^2dsdt.$$

On the other hand,

$$\begin{aligned}I_1+I_2+I_5&=\int_0^T\sum_{K\in\mathcal{T}_h}\sum_{e\subset\partial K\bigcap\mathcal{E}_\mathcal{I}}\int_e\left(\mathbf{n}_K\times\frac{\mathbf{E}_h^{int(K)}+\mathbf{E}_h^{ext(K)}}{2}\cdot\mathbf{H}_h^{int(K)}-\mathbf{n}_K\times\frac{\mathbf{H}_h^{int(K)}+\mathbf{H}_h^{ext(K)}}{2}\cdot\mathbf{E}_h^{int(K)}\right)dsdt\\ &\quad+\frac{1}{2}\int_0^T\sum_{e\subset\mathcal{E}_\mathcal{I}}\int_e\left(|[\mathbf{H}_h(\mathbf{x},t)]_T|^2+|[\mathbf{E}_h(\mathbf{x},t)]_T|^2\right)dsdt-\int_0^T\sum_{K\in\mathcal{T}_h}\sum_{e\subset\partial K\bigcap\mathcal{E}_\mathcal{I}}\int_e\mathbf{n}\times\mathbf{E}_h^{int(K)}\cdot\mathbf{H}_h^{int(K)}dsdt\\ &=\frac{1}{2}\int_0^T\sum_{e\subset\mathcal{E}_\mathcal{I}}\int_e\left(|[\mathbf{H}_h(\mathbf{x},t)]_T|^2+|[\mathbf{E}_h(\mathbf{x},t)]_T|^2\right)dsdt.\end{aligned}$$

Then we have

$$I_1+I_2+I_3+I_4+I_5=\frac{1}{2}\int_0^T\sum_{e\subset\mathcal{E}_\mathcal{I}}\int_e\left(|[\mathbf{H}_h(\mathbf{x},t)]_T|^2+|[\mathbf{E}_h(\mathbf{x},t)]_T|^2\right)dsdt+\int_0^T\sum_{e\subset\mathcal{E}_\mathcal{D}}\int_e|\mathbf{n}\times\mathbf{E}_h^{int}|^2dsdt.$$

which, together with (3.4) and (3.5), completes the proof. □

Definition 3.1. A function $\beta(t)$ is called a positive definite function if $\beta\in L_{1,loc}(\overline{R}_+)$ and satisfies

$$\int_0^T\int_0^t\beta(t-\tau)\phi(\tau)d\tau\phi(t)dt\geqslant 0\quad\forall T>0,\phi\in C([0,T]).$$

According to ((1.3), [19]), we have

Lemma 3.2. *A function β is positive definite if and only if*

$$Re\hat{\beta}(\theta) = \int_0^{\infty} \beta(t)\cos(\theta t)dt \geqslant 0, \quad \forall \theta \in R,$$

where $\hat{\beta}$ denotes the Laplace transform of β.

Lemma 3.3 (*Gronwall's Lemma*). *Suppose that ϕ is a nonnegative continuous function such that*

$$\phi(t) \leqslant a + b\int_0^t \phi(s)ds, \quad \text{for} \quad t > 0,$$

where a and b are nonnegative constants. Then

$$\phi(t) \leqslant ae^{bt}.$$

Proposition 3.1. *Let $\mathbf{U}_h = (\mathbf{H}_h, \mathbf{E}_h)$ be the solution of (2.12), (2.13) . Then, for any $T \in (0, T_0]$,*

$$\mu\|\mathbf{H}_h(\mathbf{x},T)\|^2 + \epsilon\|\mathbf{E}_h(\mathbf{x},T)\|^2 + \Theta_{T,T_h}(\mathbf{U}_h) \leqslant C(\mu\|\mathbf{H}_h(\mathbf{x},0)\|^2 + \epsilon\|\mathbf{E}_h(\mathbf{x},0)\|^2). \tag{3.6}$$

Here C is a constant dependent of T_0 if f is bounded on $(0,T_0]$, and $C = 1$ if f is positive definite.

Proof. First assume that $f(t)$ is bounded in $(0,T_0]$, i.e., there is a positive constant C_f such that

$$|f| \leqslant C_f \quad \text{in } (0, T_0].$$

According to (2.3),

$$\int_0^T \int_\Omega \mathbf{J}(\mathbf{E_h},t)\cdot\mathbf{E}_h(\mathbf{x},t)d\mathbf{x}dt = c\int_0^T \|\mathbf{E_h}(\mathbf{x},t)\|^2 dt + \int_0^T \int_\Omega \int_0^t f(t-\tau)\mathbf{E_h}(\mathbf{x},\tau)d\tau\cdot\mathbf{E_h}(\mathbf{x},t)d\mathbf{x}dt. \tag{3.7}$$

Since $B_h(\mathbf{U}_h, \mathbf{U}_h; T) = 0$ by (3.1), recalling Lemma 3.1, we get

$$\frac{1}{2}\left(\mu\|\mathbf{H}_h(\mathbf{x},T)\|^2 + \epsilon\|\mathbf{E}_h(\mathbf{x},T)\|^2\right) + \frac{1}{2}\Theta_{T,T_h}(\mathbf{U}_h) + c\int_0^T \|\mathbf{E_h}(\mathbf{x},t)\|^2 dt$$
$$\leqslant \frac{1}{2}\left(\mu\|\mathbf{H}_h(\mathbf{x},0)\|^2 + \epsilon\|\mathbf{E}_h(\mathbf{x},0)\|^2\right) + \left|\int_0^T \int_\Omega \int_0^t f(t-\tau)\mathbf{E_h}(\mathbf{x},\tau)d\tau\cdot\mathbf{E_h}(\mathbf{x},t)d\mathbf{x}dt\right|.$$

By using the Hölder inequality, we have

$$\mu\|\mathbf{H}_h(\mathbf{x},T)\|^2 + \epsilon\|\mathbf{E}_h(\mathbf{x},T)\|^2 + \Theta_{T,T_h}(\mathbf{U}_h) + 2c\int_0^T \|\mathbf{E}_h(\mathbf{x},t)\|^2 dt$$
$$\leqslant \mu\|\mathbf{H}_h(\mathbf{x},0)\|^2 + \epsilon\|\mathbf{E}_h(\mathbf{x},0)\|^2 + 2C_f\int_0^T\int_0^t \frac{1}{2}\left(\|\mathbf{E}_h(x,\tau)\|^2 + \|\mathbf{E}_h(x,t)\|^2\right)d\tau dt$$
$$\leqslant \mu\|\mathbf{H}_h(\mathbf{x},0)\|^2 + \epsilon\|\mathbf{E}_h(\mathbf{x},0)\|^2 + 2C_fT\int_0^T \|\mathbf{E}_h(x,t)\|^2 dt \leqslant \mu\|\mathbf{H}_h(\mathbf{x},0)\|^2 + \epsilon\|\mathbf{E}_h(\mathbf{x},0)\|^2 + 2C_fT_0\int_0^T \|\mathbf{E}_h(x,t)\|^2 dt.$$

Since c is a nonnegative constant, the implementation of the Gronwall's inequality leads to (3.6) with $C = C(T_0)$.

On the other hand, if f is positive definite, then (3.7) implies

$$\int_0^T \int_\Omega \mathbf{J}(\mathbf{E}_h,t)\cdot\mathbf{E}_h(\mathbf{x},t)d\mathbf{x}dt = c\int_0^T \|\mathbf{E}_h(\mathbf{x},t)\|^2 dt + \int_\Omega\int_0^T\int_0^t f(t-\tau)\mathbf{E}_h(\mathbf{x},\tau)d\tau\cdot\mathbf{E}_h(\mathbf{x},t)dtd\mathbf{x}$$
$$\geqslant c\int_0^T \|\mathbf{E}_h(\mathbf{x},t)\|^2 dt \geqslant 0. \tag{3.8}$$

Since $B_h(\mathbf{U}_h, \mathbf{U}_h; T) = 0$, the conclusion follows by applying (3.8) to (3.3). □

Now we turn to the error estimate of our approach. We first introduce two approximation lemmas.

Lemma 3.4. *Let $u \in (H^{k+1}(K))^3$ satisfying $\nabla\cdot u = 0$, and $\mathbb{P}_h u$ its L^2-projection into $\overline{\mathbf{V}}_{h,0}^k|_K$. Then*

$$\|u - \mathbb{P}_h u\|_{0,K} \leqslant Ch^{k+1}|u|_{k+1,K}, \quad \|u - \mathbb{P}_h u\|_{0,\partial K} \leqslant Ch^{k+1/2}|u|_{k+1,K}.$$

See Lemma 2.3 [6].

Lemma 3.5. *Let $u \in (H^{k+1}(K))^3$, and $\mathbb{P}_h u$ its L^2-projection into $\overline{\mathbf{V}}_h^k|_K$. Then*

$$\|u - \mathbb{P}_h u\|_{0,K} \leqslant Ch^{k+1}|u|_{k+1,K}, \quad \|u - \mathbb{P}_h u\|_{0,\partial K} \leqslant Ch^{k+1/2}|u|_{k+1,K}.$$

Now we state the main result of this section.

Proposition 3.2. *Let* $\mathbf{U} = (\mathbf{H}, \mathbf{E})$ *be the exact solution of (2.1), (2.2) with the boundary condition (2.4) and initial condition (2.5), and* $\mathbf{U}_h = (\mathbf{H}_h, \mathbf{E}_h)$ *the solution of (2.12), (2.13) in* $\mathbf{V}_h^k$*. Then for any* $T \in (0, T_0]$*,*

$$\mu\|(\mathbf{H}-\mathbf{H}_h)(\cdot,T)\| + \epsilon\|(\mathbf{E}-\mathbf{E}_h)(\cdot,T)\| \leqslant Ch^{k+1/2}(|||\mathbf{H}|||_{k+1} + |||\mathbf{E}|||_{k+1}),$$

where $|||\mathbf{H}|||_{k+1}^2 = \int_0^T \|H(\cdot,t)\|_{k+1}^2 dt$*. Here C is a constant independent of h, but dependent on* T_0 *if f(t) is bounded in* $(0,T_0]$*, and independent of both* T_0 *and h if f(t) is positive definite.*

Proof. Since the flux $\mathbf{h}(\mathbf{U}_h^{ext(K)}, \mathbf{U}_h^{int(K)}, \mathbf{n}_K)$ is consistent with $\mathbf{f}(U)\cdot n_K$, we have

$$B_h(\mathbf{U}, \mathbf{v}_h; T) = 0 \quad \forall \mathbf{v}_h(\cdot,t) \in \mathbf{V}_h^k, \quad \forall t \in (0,T), \quad \forall T \in (0, T_0]. \tag{3.9}$$

Subtracting (3.1) from (3.9) leads to the error equation

$$B_h(e, \mathbf{v}_h; T) = 0 \quad \forall \mathbf{v}_h(\cdot,t) \in \mathbf{V}_h^k, \quad \forall t \in (0,T), \quad \forall T \in (0, T_0], \tag{3.10}$$

where $e = \mathbf{U} - \mathbf{U}_h$. Rewrite

$$e = \mathbf{U} - \mathbb{P}_h(\mathbf{U}) + \mathbb{P}_h(\mathbf{U}) - \mathbf{U}_h = \mathbf{R} - \theta,$$

where $\mathbb{P}_h(\mathbf{U}) = (\mathbb{P}_h(\mathbf{H}), \mathbb{P}_h(\mathbf{E}))^T$, with $\mathbb{P}_h(\mathbf{H})$ and $\mathbb{P}_h(\mathbf{E})$ the L^2-projection of the functions $\mathbf{H}$ and $\mathbf{E}$ into $\overline{\mathbf{V}}_{\mathbf{h},0}^{\mathbf{k}}$ and $\overline{\mathbf{V}}_h^k$, respectively, $\mathbf{R} = \mathbf{U} - \mathbb{P}_h(\mathbf{U}), \theta = \mathbf{U}_h - \mathbb{P}_h(\mathbf{U}) \in \mathbf{V}_h^k$. As a result,

$$B_h(\theta, \mathbf{v}_h; T) = B_h(\mathbf{R}, \mathbf{v}_h; T) \quad \forall \mathbf{v}_h(\cdot,t) \in \mathbf{V}_h^k, \quad \forall t \in (0,T), \quad \forall T \in (0, T_0]. \tag{3.11}$$

Noting that $\mathbf{U}_h(\mathbf{x}, 0) = \mathbb{P}_h(\mathbf{U}_0)$ according to (2.13), we have

$$\theta(0) = \begin{pmatrix} \mathbf{H}_h(0) - \mathbb{P}_h(\mathbf{H}_0) \\ \mathbf{E}_h(0) - \mathbb{P}_h(\mathbf{E}_0) \end{pmatrix} = \begin{pmatrix} \mathbb{P}_h(\mathbf{H}_0) - \mathbb{P}_h(\mathbf{H}_0) \\ \mathbb{P}_h(\mathbf{E}_0) - \mathbb{P}_h(\mathbf{E}_0) \end{pmatrix} = \begin{pmatrix} 0 \\ 0 \end{pmatrix}.$$

As a consequence, Lemma 3.1 yields

$$B_h(\theta, \theta; T) = \frac{1}{2}(\mu\|\theta_{\mathbf{H}}(\mathbf{x},T)\|^2 + \epsilon\|\theta_{\mathbf{E}}(\mathbf{x},T)\|^2 + \frac{1}{2}\Theta_{T,\mathcal{T}_h}(\theta) + \int_0^T \int_\Omega \mathbf{J}(\theta_{\mathbf{E}}, t)\cdot\theta_{\mathbf{E}} d\mathbf{x}dt. \tag{3.12}$$

Let $\mathbf{v}_h = \theta$ in (3.11), we have

$$\begin{aligned} B_h(\mathbf{R}, \theta; T) &= \int_0^T \int_\Omega (\mu\partial_t \mathbf{R}_{\mathbf{H}}(\mathbf{x},t)\cdot\theta_{\mathbf{H}}(\mathbf{x},t)) + \epsilon\partial_t\mathbf{R}_{\mathbf{E}}(\mathbf{x},t)\cdot\theta_{\mathbf{E}}(\mathbf{x},t))d\mathbf{x}dt - \int_0^T \int_\Omega \mathbf{f}(\mathbf{R})\cdot\nabla\theta d\mathbf{x}dt \\ &\quad + \int_0^T \sum_{K\in\mathcal{T}_h}\sum_{e\subset\partial K}\int_e \mathbf{h}(\mathbf{R}^{ext(K)}, \mathbf{R}^{int(K)}, \mathbf{n}_K)\cdot\theta(x,t)dsdt + c\int_0^T\int_\Omega \mathbf{R}_{\mathbf{E}}\cdot\theta_{\mathbf{E}}d\mathbf{x}dt \\ &\quad + \int_0^T\int_0^t f(t-\tau)\int_\Omega \mathbf{R}_{\mathbf{E}}(\mathbf{x},\tau)\cdot\theta_{\mathbf{E}}(\mathbf{x},t)d\mathbf{x}d\tau dt \\ &= \int_0^T \sum_{K\in\mathcal{T}_h}\sum_{e\subset\partial K}\int_e \mathbf{h}(\mathbf{R}^{ext(K)}, \mathbf{R}^{int(K)}, \mathbf{n}_K)\cdot\theta(\mathbf{x},t)dsdt - \int_0^T\int_\Omega \mathbf{f}(\mathbf{R})\cdot\nabla\theta d\mathbf{x}dt, \end{aligned} \tag{3.13}$$

where the orthogonal property of the L^2-projection operator $\mathbb{P}_h$ is used. Substituting the expressions of the numerical flux $\mathbf{h}$ and $\mathbf{f}(\mathbf{R})$ into (3.13), we obtain

$$\begin{aligned} B_h(\mathbf{R}, \theta; T) &= \int_0^T \sum_{K\in\mathcal{T}_h}\sum_{e\subset\partial K\bigcap\mathcal{E}_\mathcal{I}}\int_e \mathbf{n}_K \times \left(\overline{\mathbf{R}}_{\mathbf{E}} - \frac{1}{2}[\mathbf{R}_{\mathbf{H}}]_T\right)\cdot(\theta_{\mathbf{H}})^{int(K)}dsdt - \int_0^T \sum_{K\in\mathcal{T}_h}\sum_{e\subset\partial K\bigcap\mathcal{E}_\mathcal{I}}\int_e \mathbf{n}_K \\ &\quad \times\left(\overline{\mathbf{R}}_{\mathbf{H}} + \frac{1}{2}[\mathbf{R}_{\mathbf{E}}]_T\right)\cdot(\theta_{\mathbf{E}})^{int(K)}dsdt - \int_0^T \sum_{K\in\mathcal{T}_h}\sum_{e\subset\partial K\bigcap\mathcal{E}_\mathcal{D}}\int_e \mathbf{n}\times\left(\mathbf{R}_{\mathbf{H}}^{int(K)} + \mathbf{n}\times\mathbf{R}_{\mathbf{E}}^{int}\right)\cdot\theta_{\mathbf{E}}^{int(K)}dsdt \\ &\quad - \int_0^T \sum_{K\in\mathcal{T}_h}\int_K \sum_{i=1}^3 \left(\mathbf{e}_i \times \mathbf{R}_{\mathbf{E}}\cdot\frac{\partial}{\partial x_i}\theta_{\mathbf{H}} - \mathbf{e}_i\times\mathbf{R}_{\mathbf{H}}\cdot\frac{\partial}{\partial x_i}\theta_{\mathbf{E}}\right)d\mathbf{x}dt \\ &= I_1 + I_2 + I_3 + I_4, \end{aligned}$$

where

$$I_1 + I_2 = \int_0^T \sum_{e\subset\mathcal{E}_\mathcal{I}}\int_e -\overline{\mathbf{R}}_{\mathbf{E}}\cdot[\theta_{\mathbf{H}}]_T + \overline{\mathbf{R}}_{\mathbf{H}}\cdot[\theta_{\mathbf{E}}]_T + \frac{1}{2}[\mathbf{R}_{\mathbf{H}}]_T\cdot[\theta_{\mathbf{H}}]_T + \frac{1}{2}[\mathbf{R}_{\mathbf{E}}]_T\cdot[\theta_{\mathbf{E}}]_T dsdt,$$

$$I_3 + I_4 = \int_0^T \sum_{e\subset\mathcal{E}_\mathcal{D}}\int_e \left(\mathbf{R}_{\mathbf{H}}^{int} + \mathbf{n}\times\mathbf{R}_{\mathbf{E}}^{int}\right)\cdot\left(\mathbf{n}\times\theta_{\mathbf{E}}^{int(K)}\right)dsdt - \int_0^T \sum_{K\in\mathcal{T}_h}\int_K (\nabla\times\theta_{\mathbf{E}}\cdot\mathbf{R}_{\mathbf{H}} - \nabla\times\theta_{\mathbf{H}}\cdot\mathbf{R}_{\mathbf{E}})d\mathbf{x}dt.$$

Since $\nabla \times \theta_{\mathbf{E}} \in \overline{\mathbf{V}}_{h,0}^k$ and $\nabla \times \theta_{\mathbf{H}} \in \overline{\mathbf{V}}_h^k$, we have

$$B_h(\mathbf{R},\theta;T) \leqslant \int_0^T \sum_{e\subset\mathcal{E}_\mathcal{I}} \int_e |\overline{\mathbf{R}}_{\mathbf{E}}|^2 + |\overline{\mathbf{R}}_{\mathbf{H}}|^2 + \frac{1}{4}\left(|[\mathbf{R}_{\mathbf{E}}]_T|^2 + |[\mathbf{R}_{\mathbf{H}}]_T|^2\right) dsdt + \frac{1}{2}\int_0^T \sum_{e\subset\mathcal{E}_\mathcal{D}} \int_e \left(\left|\mathbf{R}_{\mathbf{H}}^{int}\right|^2 + \left|\mathbf{n}\times\mathbf{R}_{\mathbf{E}}^{int}\right|^2\right) dsdt + \frac{1}{2}\Theta_{T,T_h}(\theta), \tag{3.14}$$

by using the orthogonal property and the Young's inequality.

Assume $f(t)$ is bounded. Similar to the proof of the L^2-stability, the combination of (3.12) and (3.14) leads to

$$\begin{aligned}
&\frac{1}{2}\left(\mu\|\theta_{\mathbf{H}}(\mathbf{x},T)\|^2 + \epsilon\|\theta_{\mathbf{E}}(\mathbf{x},T)\|^2\right) + \frac{1}{2}\Theta_{T,T_h}(\theta) + c\int_0^T \|\theta_{\mathbf{E}}\|^2 dt \\
&\quad \leqslant |B_h(\mathbf{R},\theta;T)| + C_f \int_0^T \int_0^t \frac{1}{2}\left(\|\theta_{\mathbf{E}}(x,\tau)\|^2 + \|\theta_{\mathbf{E}}(x,t)\|^2\right) d\tau dt \\
&\quad \leqslant \int_0^T \sum_{e\subset\mathcal{E}_\mathcal{I}} \int_e |\overline{\mathbf{R}}_{\mathbf{E}}|^2 + |\overline{\mathbf{R}}_{\mathbf{H}}|^2 + \frac{1}{4}\left(|[\mathbf{R}_{\mathbf{E}}]_T|^2 + |[\mathbf{R}_{\mathbf{H}}]_T|^2\right) dsdt + \frac{1}{2}\int_0^T \sum_{e\subset\mathcal{E}_\mathcal{D}} \int_e \left(\left|\mathbf{R}_{\mathbf{H}}^{int}\right|^2 + \left|\mathbf{n}\times\mathbf{R}_{\mathbf{E}}^{int}\right|^2\right) dsdt \\
&\qquad + \frac{1}{2}\Theta_{T,T_h}(\theta) + C_f T_0 \int_0^T \|\theta_{\mathbf{E}}\|^2 dt,
\end{aligned} \tag{3.15}$$

where (3.7) is used again. Noting that c is a positive constant, we have

$$\begin{aligned}
\frac{1}{2}\left(\mu\|\theta_{\mathbf{H}}(\mathbf{x},T)\|^2 + \epsilon\|\theta_{\mathbf{E}}(\mathbf{x},T)\|^2\right) &\leqslant \int_0^T \sum_{e\subset\mathcal{E}_\mathcal{I}} \int_e |\overline{\mathbf{R}}_{\mathbf{E}}|^2 + |\overline{\mathbf{R}}_{\mathbf{H}}|^2 + \frac{1}{4}\left(|[\mathbf{R}_{\mathbf{E}}]_T|^2 + |[\mathbf{R}_{\mathbf{H}}]_T|^2\right) dsdt \\
&\quad + \frac{1}{2}\int_0^T \sum_{e\subset\mathcal{E}_\mathcal{D}} \int_e \left(\left|\mathbf{R}_{\mathbf{H}}^{int}\right|^2 + \left|\mathbf{n}\times\mathbf{R}_{\mathbf{E}}^{int}\right|^2\right) dsdt + CT_0\int_0^T \left(\mu\|\theta_{\mathbf{H}}(\mathbf{x},T)\|^2 + \epsilon\|\theta_{\mathbf{E}}(\mathbf{x},T)\|^2\right) dt.
\end{aligned} \tag{3.16}$$

Applying the Gronwall's inequality and the approximation results in Lemma 3.4 and 3.5, we obtain

$$\mu\|\theta_{\mathbf{H}}(\mathbf{x},T)\|^2 + \epsilon\|\theta_{\mathbf{E}}(\mathbf{x},T)\|^2 \leqslant Ch^{2k+1}\left(\||\mathbf{H}\||_{k+1}^2 + \||\mathbf{E}\||_{k+1}^2\right),$$

by (3.16). Here C is a constant independent of h, but dependent on T_0.

On the other hand, if f is positive definite, combing (3.7) and (3.12), we have

$$B_h(\theta,\theta;T) \geqslant \frac{1}{2}\left(\mu\|\theta_{\mathbf{H}}(\mathbf{x},T)\|^2 + \epsilon\|\theta_{\mathbf{E}}(\mathbf{x},T)\|^2\right) + \frac{1}{2}\Theta_{T,T_h}(\theta). \tag{3.17}$$

In terms of (3.14) and the approximation results in Lemma 3.4 and 3.5, we obtain

$$\mu\|\theta_{\mathbf{H}}(\mathbf{x},T)\|^2 + \epsilon\|\theta_{\mathbf{E}}(\mathbf{x},T)\|^2 \leqslant Ch^{2k+1}\left(\||\mathbf{H}\||_{k+1}^2 + \||\mathbf{E}\||_{k+1}^2\right),$$

where C is independent of h and T_0. To this end, our proof can be completed by using the triangular inequality, Lemma 3.4 and 3.5. □

4. Implementation in specific media

Dispersive media are ubiquitous as mentioned in Section 1. In our work we focus on three important and useful dispersive media, i.e., isotropic cold plasma, Debye medium, and Lorentz medium.

4.1. Isotropic cold plasma

The governing equation that describes electromagnetic wave propagation in isotropic non-magnetized cold electron plasma is [5,8]

$$\mu_0 \frac{\partial \mathbf{H}}{\partial t} = -\nabla\times\mathbf{E} \quad \text{in } \Omega\times(0,T_0], \tag{4.1}$$

$$\epsilon_0 \frac{\partial \mathbf{E}}{\partial t} = \nabla\times\mathbf{H} - \mathbf{J} \quad \text{in } \Omega\times(0,T_0], \tag{4.2}$$

$$\frac{\partial \mathbf{J}}{\partial t} + \nu\mathbf{J} = \epsilon_0\omega_p^2\mathbf{E} \quad \text{in } \Omega\times(0,T_0], \tag{4.3}$$

where $\mathbf{H}$ is the magnetic field, $\mathbf{E}$ is the electric field, μ_0 is the permeability of free space, ϵ_0 is the permittivity of free space, $\mathbf{J}$ is the polarization current density, ω_p is the plasma frequency, ν is the electron-neutral collision frequency, and μ_0,ϵ_0,ω_p, ν are constants. Under the assumption that the initial electron velocity is zero, the polarization current density **J** can be expressed as

$$\mathbf{J} = \mathbf{J}(\mathbf{E}, t) = \epsilon_0 \omega_p^2 \int_0^t e^{-\nu(t-\tau)} \mathbf{E}(\mathbf{x}, \tau) d\tau. \tag{4.4}$$

Substituting (4.4) into (4.2), we obtain the model problem (2.1), (2.2) with $\mu = \mu_0$, $\epsilon = \epsilon_0$, $c = 0$, $f(t) = \epsilon_0 \omega_p^2 e^{-\nu t}$.

It is straightforward to verify that $f(t) = \epsilon_0 \omega_p^2 e^{-\nu t}$ is positive definite by Lemma 3.2. As a consequence, Propositions 3.1 and 3.2 hold for this case with constant C independent of h and T_0.

4.2. Debye medium

For the single pole model of Debye, the governing equation is [14]

$$\mu_0 \frac{\partial \mathbf{H}}{\partial t} = -\nabla \times \mathbf{E} \quad \text{in } \Omega \times (0, T_0], \tag{4.5}$$

$$\epsilon_0 \epsilon_\infty \frac{\partial \mathbf{E}}{\partial t} = \nabla \times \mathbf{H} - \frac{1}{t_0}[(\epsilon_s - \epsilon_\infty)\epsilon_0 \mathbf{E} - \mathbf{P}] \quad \text{in } \Omega \times (0, T_0], \tag{4.6}$$

$$\frac{\partial \mathbf{P}}{\partial t} + \frac{1}{t_0}\mathbf{P} = \frac{(\epsilon_s - \epsilon_\infty)\epsilon_0}{t_0}\mathbf{E} \quad \text{in } \Omega \times (0, T_0], \tag{4.7}$$

where **P** is the polarization vector, ϵ_∞ is the permittivity at infinite frequency, ϵ_s is the permittivity at DC, t_0 is the relaxation time, and the rest have the same meaning as those stated previously for the isotropic cold plasma medium. Here ϵ_∞,ϵ_s and t_0 are constants and $\epsilon_\infty < \epsilon_s$. Similarly we obtain the model problem (2.1), (2.2) by substituting the expression of **P** in terms of **E** obtained from (4.7) into (4.6). Here $\mu = \mu_0$, $\epsilon = \epsilon_0 \epsilon_\infty$, $c = (\epsilon_s - \epsilon_\infty)\epsilon_0 / t_0$, $f = -\frac{\epsilon_s - \epsilon_\infty}{t_0^2} e^{-\frac{t}{t_0}}$. It is clear that c is a nonnegative constant and f is bounded by $C_f = \frac{\epsilon_s - \epsilon_\infty}{t_0^2}$. Thus L^2-stability and error estimate in Section 3 hold.

4.3. Lorentz medium

For the Lorentzian two-pole model, the problem is described by the following equation [23]

$$\epsilon_0 \epsilon_\infty \frac{\partial \mathbf{E}}{\partial t} = \nabla \times \mathbf{H} - \mathbf{J} \quad \text{in } \Omega \times (0, T_0], \tag{4.8}$$

$$\mu_0 \frac{\partial \mathbf{H}}{\partial t} = -\nabla \times \mathbf{E} \quad \text{in } \Omega \times (0, T_0], \tag{4.9}$$

$$\frac{\partial \mathbf{J}}{\partial t} = -\nu \mathbf{J} + (\epsilon_s - \epsilon_\infty)\epsilon_0 \omega_1^2 \mathbf{E} - \omega_1^2 \mathbf{P} \quad \text{in } \Omega \times (0, T_0], \tag{4.10}$$

$$\frac{\partial \mathbf{P}}{\partial t} = \mathbf{J} \quad \in \quad \Omega \times (0, T_0], \tag{4.11}$$

where, in addition to the notation defined early, ω_1 is the resonant frequency, ν is the damping coefficient and **P** is the polarization vector. According to [14], in terms of (4.10) and (4.11), we can obtain

$$\mathbf{J} = \mathbf{J}(\mathbf{E}, t) = \tilde{\beta} \int_0^t e^{-\delta(t-\tau)} \sin(\gamma - \alpha(t - \tau)) \mathbf{E}(\mathbf{x}, \tau) d\tau, \tag{4.12}$$

with $\delta = \frac{\nu}{2}$, $\alpha = \sqrt{\omega_1^2 - \delta^2}$, $\tilde{\beta} = (\epsilon_s - \epsilon_\infty)\epsilon_0 \omega_1^3 / \sqrt{\omega_1^2 - \frac{\nu^2}{4}}$, and γ is a constant such that $\cos\gamma = \delta/\omega_1$, $\sin\gamma = \alpha/\omega_1$. Substituting (4.12) into (4.8), we have the model problem (2.1), (2.2) with $\mu = \mu_0$, $\epsilon = \epsilon_0 \epsilon_\infty$, $c = 0$, $f = \tilde{\beta} e^{-\delta t} \sin(\gamma - \alpha t)$ which is bounded by $\tilde{\beta}$. Again, we have the L^2-stability and error estimate for this case as shown in Propositions 3.1 and 3.2.

5. Numerical results

In this section, numerical examples for both 2D and 3D Maxwell equations with dispersive term are given. The computational domain is $[0,1]^2$ for 2D case and $[0,1]^3$ for 3D case.

5.1. 2D numerical example

The similar error estimate for 2D Maxwell equations in dispersive media can be obtained in the same way as we have done for 3D case, by introducing the scalar and vector curl operators

$$\text{curl } \mathbf{E} = \frac{\partial E_2}{\partial x} - \frac{\partial E_1}{\partial y}, \quad \nabla \times E = \left(\frac{\partial E}{\partial y}, -\frac{\partial E}{\partial x} \right)^T.$$

To justify our theoretical analysis, we first give a 2D numerical example. Consider a 2D plasma problem [14], i.e.,

$$\begin{cases} \mu_0 \frac{\partial H_x}{\partial t} + \frac{\partial E_z}{\partial y} = R_1, \\ \mu_0 \frac{\partial H_y}{\partial t} - \frac{\partial E_z}{\partial x} = R_2, \\ \epsilon_0 \frac{\partial E_z}{\partial t} - (\frac{\partial H_y}{\partial x} - \frac{\partial H_x}{\partial y}) + J(E_z) = R_3, \end{cases}$$

where $J(E_z) = \epsilon_0 \omega_p^2 \int_0^t e^{-(t-\tau)} E_z(\mathbf{x}, \tau) d\tau$, $\mathbf{R}_i$, i = 1, 2, 3 are chosen such that the exact solution is

$$\begin{pmatrix} H_x \\ H_y \\ E_z \end{pmatrix} = 100 \begin{pmatrix} x(1-x)(1-2y)te^{-\nu t} \\ -y(1-y)(1-2x)te^{-\nu t} \\ xy(1-x)(1-y)te^{-\nu(t+(x+y)/\sqrt{2})} \end{pmatrix}.$$

For simplicity we assume that $\mu_0 = \epsilon_0 = \nu = \omega_p = 1$. The L^2-errors and their corresponding convergence rate by using our DG approach are presented in Tables 1 and 2 for $k = 1$ and $k = 2$, respectively. Here N is the number of time steps, which means that $t = N \times dt$ at the Nth step (for example, $t = 10^{-2}$ when $N = 10$, $dt = 10^{-3}$). We note that the L^2 errors are O (h^{k+1}) for both $\mathbf{H}_h$ and $E_{z,h}$, which are better than our theoretical prediction. Fig. 1 shows the point-wise errors of $H_{x,h}$ under 8×8 meshes when $dt = 0.1$ and $N = 10$ ($k = 1$, on the top and $k = 2$, on the bottom), respectively.

5.2. 3D numerical example

We consider the following 3D Maxwell equations

$$\begin{cases} \mu_0 \frac{\partial \mathbf{H}}{\partial t} + \nabla \times \mathbf{E} = R_1, \\ \epsilon_0 \frac{\partial \mathbf{E}}{\partial t} - \nabla \times \mathbf{H} + \mathbf{J}(\mathbf{E}) = R_2. \end{cases}$$

with dispersive term $\mathbf{J}(\mathbf{E}) = \int_0^t e^{-(t-\tau)} \mathbf{E}(\mathbf{x}, \tau) d\tau$. Here $\mathbf{R}_i$,i = 1,2 are chosen such that the exact solution is

$$\mathbf{E} = \begin{pmatrix} (y-y^2)(z-z^2) \\ (x-x^2)(z-z^2) \\ (x-x^2)(y-y^2) \end{pmatrix} te^{-(t+x+y+z)} \quad \mathbf{H} = \begin{pmatrix} y-z \\ z-x \\ x-y \end{pmatrix} te^{-(t+x+y+z)}.$$

Table 1
The numerical results for $k = 1$, $dt = 10^{-3}$, 2D case.

	Time steps	$\|E_z - E_{z,h}\|_0$	Order	Relative error in percentage	$\|\mathbf{H} - \mathbf{H}_h\|_0$	Order	Relative error in percentage
4 × 4 mesh	N = 1	1.1311e−4		6.6480	9.0620e−4		6.0851
	N = 10	1.1374e−3		6.7458	8.9830e−3		6.0866
	N = 100	1.5058e−2		9.7714	8.3736e−2		6.2079
	N = 1000	1.2447e−1		19.8662	6.4254e−1		11.7165
8 × 8 mesh	N = 1	2.9622e−5	1.9330	1.7411	2.3117e−4	1.9709	1.5523
	N = 10	3.0053e−4		1.7823	2.2922e−3		1.5531
	N = 100	3.5833e−3		2.3253	2.1674e−2		1.6069
	N = 1000	2.5288e−2		4.0361	2.1756e−1		3.9671
16 × 16 mesh	N = 1	7.4943e−6	1.9828	0.4405	5.8079e−5	1.9929	0.3899
	N = 10	7.6719e−5		0.4550	5.7628e−4		0.3904
	N = 100	8.2408e−4		0.5348	5.5471e−3		0.4112
	N = 1000	5.0402e−3		0.8045	1.1549e−2		1.2317

Table 2
The numerical results for $k = 2$, $dt = 10^{-3}$, 2D case.

	Time steps	$\|E_z - E_{z,h}\|_0$	Order	Relative error in percentage	$\|\mathbf{H} - \mathbf{H}_h\|_0$	Order	Relative error in percentage
4 × 4 mesh	N = 1	1.6897e−5		0.9931	9.4996e−5		0.6379
	N = 10	1.6964e−4		1.0060	9.4151e−4		0.6379
	N = 100	1.9611e−3		1.2726	8.6756e−3		0.6432
	N = 1000	7.6719e−3		1.2245	3.9141e−2		0.7137
8 × 8 mesh	N = 1	2.2016e−6	2.9401	0.1294	1.1875e−5	2.9999	0.0797
	N = 10	2.2279e−5		0.1321	1.1775e−4		0.0798
	N = 100	2.2273e−4		0.1445	1.0941e−3		0.0811
	N = 1000	8.9013e−4		0.1421	4.9033e−3		0.0894
16 × 16 mesh	N = 1	2.7836e−7	2.9835	0.0164	1.4844e−6	3.0000	0.0100
	N = 10	2.8435e−6		0.0169	1.4748e−5		0.0100
	N = 100	2.6416e−5		0.0171	1.3771e−4		0.0102
	N = 1000	1.0709e−4		0.0170	6.1096e−4		0.0111

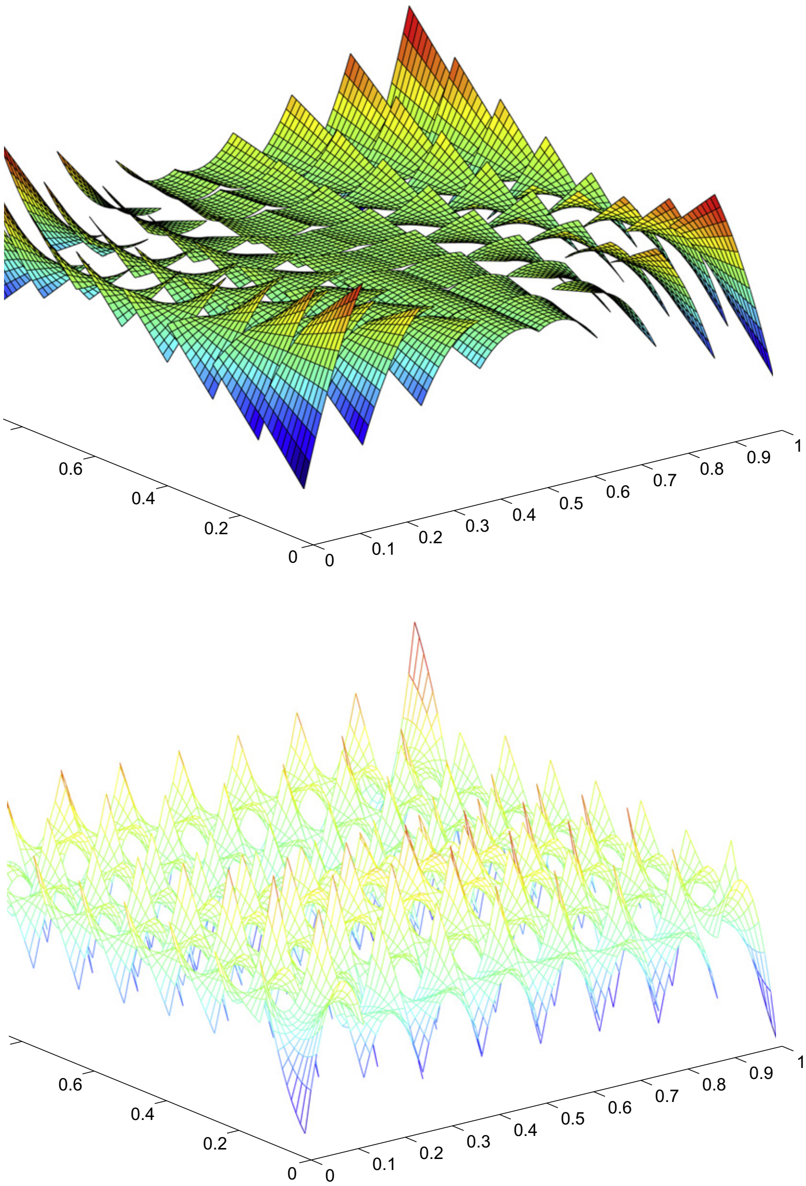

Fig. 1. The point-wise error on 8 × 8 of H_x when $k = 1$ (top) and $k = 2$ (bottom).

Table 3
The numerical results for $k = 1$, $dt = 10^{-3}$, 3D case.

	Time steps	$\|\mathbf{E}-\mathbf{E}_h\|_0$	Order	Relative error in percentage	$\|\mathbf{H}-\mathbf{H}_h\|_0$	Order	Relative error in percentage
2 × 2 × 2 mesh	N = 1	3.6392e−4		24.3005	1.9654e−3		10.7572
	N = 10	3.8547e−3		25.9717	1.9486e−2		10.9618
	N = 100	8.4417e−2		62.2341	1.7924e−1		10.8314
	N = 1000	6.8925e−1		124.98	7.5858e−1		11.2751
4 × 4 × 4 mesh	N = 1	1.1328e−4	1.6837	7.5642	5.1152e−4	1.9420	2.7998
	N = 10	1.2547e−3		8.4541	5.0731e−3		2.8018
	N = 100	2.9320e−2		21.6176	4.6982e−2		2.8391
	N = 1000	1.8520e−1		33.5814	2.1326e−1		3.1698
8 × 8 × 8 mesh	N = 1	3.0123e−5	1.9110	2.0113	1.2919e−4	1.9853	0.7071
	N = 10	3.8187e−4		2.5726	1.2823e−3		0.7082
	N = 100	8.7791e−3		6.4722	1.1981e−2		0.7240
	N = 1000	4.7418e−2		8.5982	6.0399e−2		0.8977

Table 4
The numerical results for $k = 2$, $dt = 10^{-3}$, 3D case.

	Time steps	$\|\mathbf{E}-\mathbf{E}_h\|_0$	Order	Relative error in percentage	$\|\mathbf{H}-\mathbf{H}_h\|_0$	Order	Relative error in percentage
$2\times2\times2$ mesh	N = 1	1.1547e−6		7.7123	2.2855e−6		1.2509
	N = 10	1.1649e−5		7.8527	2.2660e−5		1.2515
	N = 100	1.6385e−4		12.0848	2.1130e−4		1.2770
	N = 1000	1.0417e−3		18.8973	9.8860e−4		1.4694
$4\times4\times4$ mesh	N = 1	1.8705e−7	2.6258	1.2490	2.9928e−7	2.9329	0.1638
	N = 10	1.9269e−6		1.2983	2.9744e−6		0.1643
	N = 100	2.7356e−5		2.0168	2.9398e−5		0.1777
	N = 1000	1.4766e−4		2.6774	1.4093e−4		0.2095
$8\times8\times8$ mesh	N = 1	2.4947e−8	2.9065	0.1666	3.7857e−8	2.9829	0.0207
	N = 10	2.7139e−7		0.1829	3.8016e−7		0.0209
	N = 100	3.8244e−6		0.2819	3.9886e−6		0.0241
	N = 1000	1.8542e−5		0.3362	1.8539e−5		0.0276

The L^2-errors and their corresponding convergence order are shown in Tables 3 and 4 for $k = 1$ and $k = 2$, respectively. As in the 2D case, we observe that the convergence rate of both $\mathbf{H}_h$ and $\mathbf{E}_h$ in L^2 norm is $O(h^{k+1})$, which is better than the theoretical analysis.

6. Concluding remarks

Discontinuous Galerkin methods are very important approaches for solving Maxwell equations. It is also a feasible numerical method when dispersive media are involved. In this paper, we proved that the DG method with an up-winding flux for solving Maxwell equations in three different dispersive media (e.g., isotropic cold plasma, Debye and Lorentz media) has an accuracy of $O(h^{k+\frac{1}{2}})$ in the L^2-norm. However, it seems to be hard to analyze the error for the fully discrete formulation when the continuous finite element method is used in time discretization. A high-order and stable fully discrete DG scheme for Maxwell equations in dispersive media is our ongoing work. Furthermore, we will also consider other dispersive media in future.

References

[1] D.N. Arnold, F. Brezzi, B. Cockburn, L.D. Marini, Unified analysis of discontinuous Galerkin methods for elliptic problems, SIAM J. Numer. Anal. 39 (5) (2002) 1749–1779.
[2] D. Boffi, P. Fernandes, L. Gastaldi, I. Perugia, Computational models of electromagnetic resonators: analysis of edge element approximation, SIAM J. Numer. Anal. 36 (1999) 1264–1290.
[3] A. Buffa, R. Hiptmair, T. Von Petersdorff, C. Schwab, Boundary element methods for Maxwell transmission problems in Lipschitz domains, Numer. Math. 95 (2003) 459–485.
[4] M.H. Chen, B. Cockburn, F. Reitich, High-order RKDG methods for Computational electromagnetics, J. Sci. Comput. 22–23 (2005) 205–226.
[5] Q. Chen, M. Katsurai, P.H. Aoyagi, An FDTD formulation for dispersive media using a current density, IEEE Trans. Antennas Propag. 46 (1998) 739–1746.
[6] B. Cockburn, F.Y. Li, C.W. Shu, Locally divergence-free discontinuous Galerkin methods for the Maxwell equations, J. Comput. Phys. 194 (2004) 588–610.
[7] B. Cockburn, C.W. Shu, Runge–Kutta Discontinuous Galerkin methods for convection-dominated problems, J. Sci. Comput. 16 (2001) 173–261.
[8] S.A. Cummer, An analysis of new and existing FDTD methods for isotropic cold plasma and a method for improving their accuracy, IEEE Trans. Antennas Propag. 45 (1997) 392–400.
[9] L. Demkowicz, P. Monk, L. Vardapetyan, W. Rachowicz, de Rham diagram for hp finite element spaces, Comput. Math. Appl. 39 (2000) 29–38.
[10] J.S. Hesthaven, T. Warburton, Nodal high-order methods on unstructured grids, I: time-domain solution of Maxwell equations, J. Comput. Phys. 181 (2002) 186–221.
[11] R. Hiptmair, Finite elements in computational electromagnetism, Acta Numer. 11 (2002) 237–339.
[12] Y.Q. Huang, J. Li, Interior penalty discontinuous Galerkin method for Maxwell's equations in cold plasma, J. Sci. Comput. 41 (2009) 321–340.
[13] D. Jiao, J.M. Jin, Time-domain finite-element modeling of dispersive media, IEEE Microwave Wireless Compon. Lett. 11 (2001) 220–223.
[14] J. Li, Error analysis of fully discrete mixed finite element schemes for 3D Maxwell's equations in dispersive media, Comput. Methods Appl. Mech. Eng. 196 (2007) 3081–3094.
[15] J. Li, Error analysis of finite element methods for 3D Maxwell's equations in dispersive media, J. Comput. Appl. Math. 188 (2006) 107–120.
[16] J. Li, Y. Chen, Analysis of a time-domain finite element method for 3D Maxwell's equations in dispersive media, Comput. Methods Appl. Mech. Eng. 195 (2006) 4220–4229.
[17] J. Li, A. Wood, Finite element analysis for wave propagation in double negative metamaterials, J. Sci. Comput., 32(2), pp. 263–284.
[18] T. Lu, P. Zhang, W. Cai, Discontinuous Galerkin methods for dispersive and lossy Maxwell's equations and PML boundary conditions, J. Comput. Phys. 200 (2004) 549–580.
[19] W. Melean, V. Thomée, Numerical solution of an evolution equation with a positive-type memory term, J. Aust. Math. Soc., Ser. B 35 (1993) 23–70.
[20] P. Monk, A mixed method for approximating Maxwell's equations, SIAM Numer. Anal. 28 (1991) 1610–1634.
[21] I. Perugia, D. Schötzau, P. Monk, Stabilized interior penalty methods for the time-harmonic Maxwell equations, Comput. Methods Appl. Mech. Eng. 191 (41) (2002) 4675–4697.
[22] L. Vardapetyan, L. Demkowicz, hp-adaptive finite elements in electromagnetics, Comput. Methods Appl. Mech. Eng. 169 (1999) 331–344.
[23] J.L. Young, A. Kittichartphayak, Y.M. Kwork, D. Sullivan, On the dispersion errors related to $(FD)^2$ TD type scheme, IEEE Trans. Microwave Theor. Tech. 43 (1993) 1902–1910.